

Spatiotemporal coherent control using shaped, temporally focused pulses

Dan Oron and Yaron Silberberg

*Department of physics of Complex Systems, The Weizmann Institute of Science, Rehovot
76100, Israel*

dan.oron@weizmann.ac.il

Abstract: In most coherent control experiments with femtosecond pulses, the temporal shape of the pulses is maintained throughout the interaction region. Here we show how pulses can be controlled such that their shapes vary rapidly even when propagating very short distances of a few micrometers. This changing pulse shape has a significant effect on coherent nonlinear optical processes. Here we study third-harmonic generation induced by a coherently controlled excitation pulse whose temporal profile changes along the axial coordinate. We show how such manipulations can be used to improve the axial resolution in a multiphoton optical microscope.

© 2005 Optical Society of America

OCIS codes: (190.4180) Multiphoton processes; (190.7110) Ultrafast nonlinear optics

References and links

1. A. Assion et al., "Control of chemical reactions by feedback-optimized pulse-shaped femtosecond laser pulses," *Science* **282**, 919 (1998).
2. N. Dudovich, D. Oron, Y. Silberberg, "Single-pulse coherently-controlled nonlinear Raman spectroscopy and microscopy," *Nature* **418**, 512 (2002).
3. P. Tian, D. Keusters, Y. Suzuki, W.S. Warren, "Femtosecond phase-coherent two dimensional spectroscopy," *Science* **300**, 1553 (2003).
4. D. Felinto, L.H. Acioli, S.S. Vianna, "Temporal coherent control of a sequential transition in rubidium atoms," *Opt. Lett.* **25**, 917 (2000); N. Dudovich, D. Oron, Y. Silberberg, "Coherent transient enhancement of optically induced resonant transitions," *Phys. Rev. Lett.* **88**, 123004 (2002).
5. T. Feurer, J.C. Vaughan, K.A. Nelson, "Spatiotemporal coherent control of lattice vibrational waves," *Science*, **299**, 374 (2003).
6. D. Oron, E. Tal, Y. Silberberg, "Scanningless depth resolved microscopy," *Opt. Express* **13**, 1468 (2005), <http://www.opticsexpress.org/abstract.cfm?URI=OPEX-13-5-1468>.
7. E. Tal, D. Oron, Y. Silberberg, "Improved depth resolution in video-rate line-scanning multiphoton microscopy using temporal focusing," *Opt. Lett.* **30**, 1686 (2005).
8. G. Zhu, J. van Howe, M. Durst, W. Zipfel, C. Xu, "Simultaneous spatial and temporal focusing of femtosecond pulses," *Opt. Express* **13**, 2153-2159 (2005), <http://www.opticsexpress.org/abstract.cfm?URI=OPEX-13-6-2153>.
9. T. Brixner, G. Gerber, "Femtosecond polarization pulse shaping," *Opt. Lett.* **26**, 557 (2001); T. Brixner, G. Kramper, P. Niklaus, G. Gerber, "Generation and characterization of polarization shaped femtosecond laser pulses," *Appl. Phys. B* **74**, S133 (2002).
10. Y. Barad, H. Eisenberg, M. Horowitz, and Y. Silberberg, "Nonlinear scanning laser microscopy by third harmonic generation," *Appl. Phys. Lett.* **70**, 922 (1997).
11. D. Oron, Y. Silberberg, "Harmonic generation with temporally focused ultrashort pulses," Accepted for publication in *J. Opt. Soc. Am. B* (2005).
12. R. Boyd, *Nonlinear Optics*, (Academic press, New York, 1992).
13. E. Frumker, D. Oron, D. Mandelik, Y. Silberberg, "Femtosecond pulse shape modulation at kilohertz rates," *Opt. Lett.* **29**, 890 (2004).
14. D. Meshulach, Y. Silberberg, "Coherent quantum control of two-photon transitions by a femtosecond laser pulse," *Nature* **396**, 239 (1998).

15. P.B. Corkum, N.H. Burnett, M.Y. Ivanov, "Subfemtosecond pulses," *Opt. Lett.* **19**, 1870 (1994); M. Ivanov, P.B. Corkum, T. Zuo, A. Bandrauk, "Routes to control of intense-field atomic polarizability," *Phys. Rev. Lett.* **74**, 2933 (1995).
-

1. Introduction

The yield of a nonlinear optical process strongly depends on the temporal profile of the excitation pulse. This has been the basis for numerous applications of ultrafast pulse shaping techniques to quantum control of such processes. Among other applications, shaped ultrashort pulses have been used to control chemical reactions [1] and for enhanced spectroscopy and microscopy schemes [2, 3]. In most coherent control experiments to date, the shape of the pulse remained practically invariant throughout the interaction. Indeed, propagation effects, and in particular group-velocity dispersion (GVD) might have affected slightly the pulse shapes in some of the experiments. Dispersion induced by long propagation through a resonant system might even have a strong effect on pulse shapes in certain cases [4]. However, these changes were mostly treated as undesirable, spurious effects.

Here we show that one could tailor not only the shape of pulses, but also the way and the rate in which the pulse-shape changes along the propagation direction. Most importantly, we can induce significant changes in pulse shapes on a scale of just a few micrometers, much faster than what can be induced, for example, through material dispersion. The core idea for the rapidly varying pulse shape is the introduction of geometrical dispersion, as was recently demonstrated in the formation of temporally focused pulses [6, 7, 8]. Here we combine temporal focusing with phase-and-polarization Fourier-domain pulse shaping. This results in an excitation pulse whose temporal profile and polarization properties change as it propagates over a length scale of a few microns.

We show that this ability can be applied to control coherent nonlinear interactions. In such interactions, the yield depends strongly on the spatial variation of the excitation field. The ability to generate spatially varying temporal waveforms could enable a much higher degree of controllability on such processes. Indeed, a transverse spatiotemporal pulse shaping apparatus, based on a two-dimensional pulse shaping device has recently been used for controlled excitation of terahertz phonon-polaritons [5]. In this experiment, the incoming beam is practically split into a number of beamlets, and the spectral phase of each beamlet is controlled independently. In contrast, our work describes longitudinal shape control along the pulse propagation direction.

The key element in our scheme is a temporal lens which is a time-domain analog of the conventional lens. An ultrashort pulse impinging upon it emerges temporally stretched, but then it experiences second order dispersion of geometrical origin as it propagates. This results in rapid recompression of the pulse, which reaches its highest peak intensity at the temporal focal plane and then stretches as it further propagates. The experimental setup of the temporal lens, practically comprised of a diffraction grating and a high magnification telescope, is shown in Fig. 1. The temporal rayleigh range is equal to the spatial rayleigh range of the microscope objective. Further details can be found in Refs [6, 7].

Temporal focusing is, in fact, a crude form of spatiotemporal control, where the pulse chirp is varied over the Rayleigh range of the objective lens. It does not, however, enable generation of controlled temporal waveforms. To do so we introduce a phase-and-polarization spatial light modulator [9] into the Fourier plane of the temporal lens, as shown in Fig. 1. At the temporal focal plane, where the pulse experiences no geometrical dispersion, its temporal profile is completely determined by the spectral phases and polarizations applied to the spatial light modulator. Out of focus, however, the generated waveform is also influenced by the amount of geometrical dispersion, and thus can have significantly different properties.

To demonstrate the effects of this control scheme we choose a very simple model system - third-harmonic generation (THG) from a glass-air interface. THG induced by near-infrared pulses is typically an instantaneous third-order nonlinear process. Due to phase matching conditions, THG appears only from interfaces or small inclusions when excited by focused gaussian beams [10]. We have recently shown that this also applies for THG excited by temporally focused beams [11]. THG is also highly sensitive to the polarization of the excitation pulse. From an isotropic sample, linearly polarized illumination yields linearly polarized THG, whereas circularly polarized illumination generates no THG due to the Kleinmann symmetry [12]. In the following we show how by generating spatially varying field and polarization transients we can improve the axial resolution in THG microscopy.

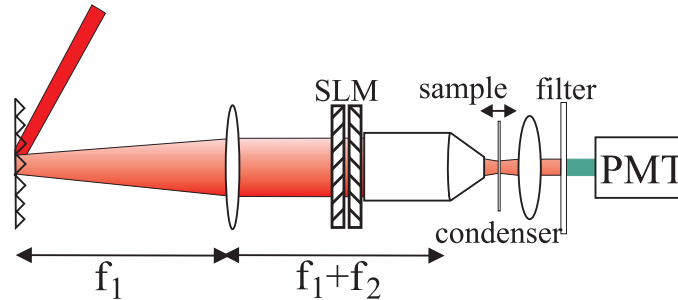


Fig. 1. Experimental setup of our coherent control apparatus: The input beam impinges upon a grating, aligned perpendicular to the optic axis of a high magnification telescope, comprised of a cylindrical lens and the microscope objective (with focal lengths f_1 and f_2 , respectively). A phase-and-polarization SLM is placed at the Fourier plane, next to the microscope objective. The sample is mounted on a piezoelectric stage. The integrated THG signal is collected in the forward direction, filtered, and measured by a photomultiplier tube.

2. Experimental

The optical setup used in the experiments is detailed in Fig. 1. It consists of an ultrafast laser source emitting 100fs pulses at 1500nm. The pulses impinge on a 600l/mm grating at an angle of about 70° chosen so that the pulse central frequency is diffracted perpendicular to the grating surface. The spectrally spread pulse is collimated by a cylindrical lens ($f=30\text{cm}$), passed through a phase-and-polarization liquid crystal SLM and focused into the sample by a NA=1.3 oil immersion objective lens. This results in a temporally focused illuminated line of about $20\mu\text{m}\times 0.7\mu\text{m}$ [7, 11]. The sample, a glass slide, is mounted on a piezoelectric stage enabling us to perform Z-scans. The THG signal is collected by a NA=0.6 lens, passed through a polarizer (when required), a spectral filter rejecting the fundamental excitation light and measured by a photomultiplier tube and a lock-in amplifier.

2.1. Phase control of temporally focused pulses

The result of a Z-scan through the glass-air interface, without applying a spectral phase function on the SLM, is plotted in Fig. 2 (blue line). This measurement reflects the axial resolution of the THG microscope, which is typically equal to the rayleigh range of the microscope objective [12]. In this case this results in a FWHM of about $3.6\mu\text{m}$. Along with this measurement we plot a Z-scan when a π phase step at the pulse central frequency was applied to the SLM (red line). This results in a significant decrease in the pulse peak intensity at the temporal focal plane, and accordingly, the THG intensity drops by a factor of 12. As can be seen, at large values of $|z|$, the

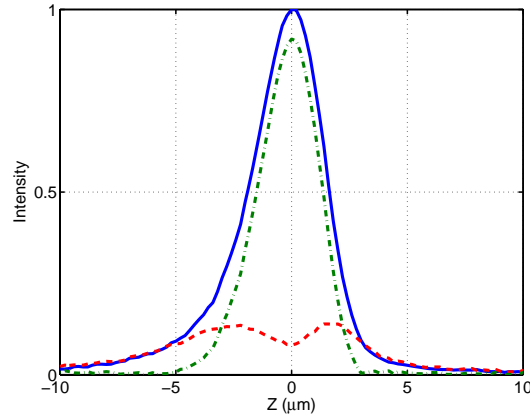


Fig. 2. Enhancement of the cross-sectioning capability by phase-only control: Plotted are the measured Z-scans with either no phase applied to the SLM (solid blue line) And with a π phase step applied at the center frequency of the pulse (dashed red line). The difference between the two (dashdotted green line) exhibits better cross-sectioning and complete rejection of the response at the tails.

two lines overlap, reflecting the fact that the dispersion overwhelms the narrow-band spectral phase change. What is surprising is the response at small values of $|z|$, where the THG signal increases with the introduction of dispersion, regardless of its sign. This effect can be readily understood when looking at the temporal profile of the pulse at the temporal focal plane and at the FWHM of the unshaped Z-scan.

The temporal profile of the unshaped pulses are shown in Fig. 3(a), and show the expected dispersive behavior, i.e. pulse broadening with the addition of dispersion. Temporal profiles with an applied π step are shown in Fig. 3(b). Surprisingly, the addition of dispersion causes an increase in the peak intensity and hence in the THG yield. The asymmetry between the two peaks (at $t=-100$ fs and at $t=100$ fs) is due to the sign of the dispersion, but since the initial profile is symmetric the increase in the THG yield is expected to be independent of the dispersion sign. Overall, when subtracting the two measured lines shown in Fig. 2, we obtain the green line, which has a FWHM smaller by 15% than the measured one, and has no response at the wings. This sort of a measurement can be easily realized experimentally by performing a lock-in measurement over rapidly varying pulse shapes [13], and results in improved background rejection, particularly of the tails of the depth response, at a very small (less than 10%) cost to the $z=0$ response.

2.2. Phase-and-polarization control of temporally focused pulses

In a second experiment we take advantage of the polarization dependence of THG to achieve, in a similar manner, a higher improvement of the depth resolution, albeit at a higher cost to the signal level. Using the SLM we shift the polarization of the upper half of the pulse spectrum from the horizontal axis to the vertical one. Moreover, an arbitrary additional phase $\exp(i\phi)$ is applied to the vertically polarized component. At the temporal focal plane, where the pulse experiences no geometrical dispersion, the vertically polarized and the horizontally polarized components temporally overlap. Thus, at $z=0$ the excitation polarization is dictated by the value of ϕ , leading to nearly linear polarization (at $\pm 45^\circ$) for $\phi = 0, \pi$ and to nearly circular polarization for $\phi = \pi/2, 3\pi/2$. At large values of $|z|$ the two polarization components do not temporally overlap. At small values, of the order of the rayleigh range, the relative phase of the two po-

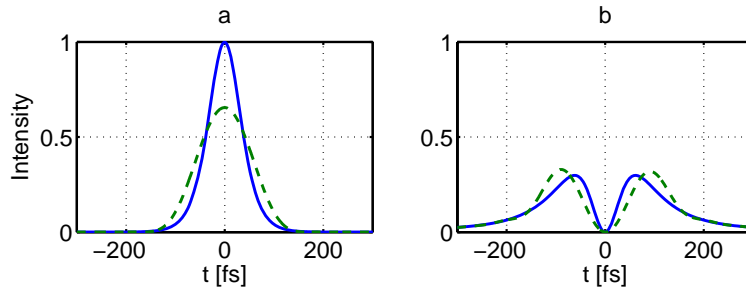


Fig. 3. The effect of dispersion on an unshaped pulse (a) and on the π step pulse (b). Shown are the temporal profiles of the pulses at $z=0$ (solid blue lines) and at the FWHM of the THG response (dashed green lines). As can be seen, dispersion reduces the THG yield for unshaped pulses but increases the THG yield from the π step pulse regardless of its sign.

larization components is modified by the geometric dispersion. Thus, if at $z=0$ the polarization is linear, it is flanked on both positive and negative values of z with regions of nearly circular polarization and vice versa.

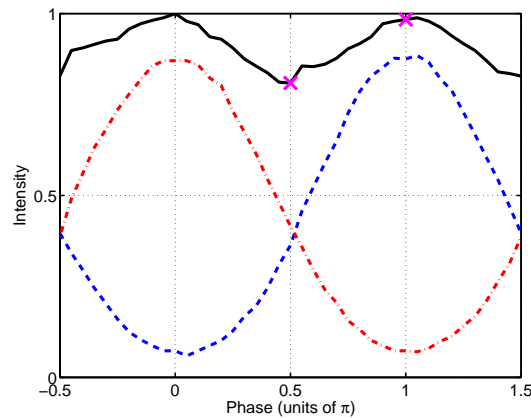


Fig. 4. Control of THG by modification of the transient polarization at the temporal focal plane: THG signal as a function of the relative phase applied to the vertically polarized and horizontally polarized components of the excitation pulse without a polarizer (solid black line), with a polarizer at 45° (dashdotted red line) and with a polarizer at -45° (dashed blue line).

This effect is readily observed when measuring the total THG signal at $z=0$ as a function of ϕ , as plotted in Fig. 4 (black line). Not surprisingly, the THG yield is highest when the polarization at $z=0$ is linear and lowest when it is circular. This is due to the fact that no THG is generated for circularly polarized light. Inserting a polarizer between the sample and the detector at $+45^\circ$ (red line) and at -45° (blue line) one can indeed see that at the peaks the THG is indeed oriented predominantly along the polarization axis of the fundamental at $z=0$.

Performing two Z-scans, at $\phi = \pi$ and at $\phi = \pi/2$, denoted by Xs in Fig. 4, we obtain the two graphs shown in Fig. 5. As can be seen, the measured THG signal is higher for $\phi = \pi$ only in a limited region around $z=0$. The difference between these, plotted in green, has a FWHM of $2.4\mu\text{m}$, nearly 35% less than the FWHM obtained from an unshaped pulse. The wings of the

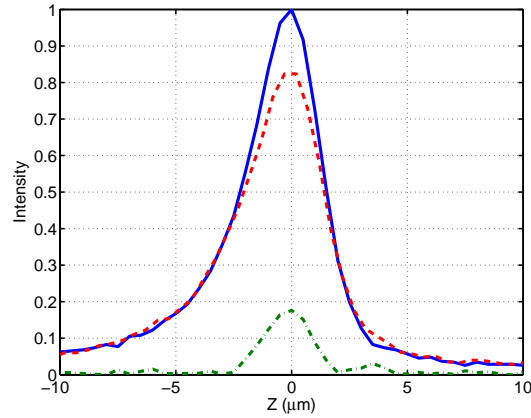


Fig. 5. Enhancement of the cross-sectioning capability by phase-and-polarization control: Plotted are the measured Z-scans with either a π relative phase between the vertical and the horizontal polarizations (solid blue line) or a $\pi/2$ relative phase (dashed red line). The difference between the two (dashdotted green line) exhibits better cross-sectioning than observed in Fig. 2.

depth response are practically eliminated beyond the FWHM of an unshaped pulse.

3. conclusion

In conclusion, we have developed a method for combined spatial and temporal control of non-linear optical interactions, which opens a variety of possible applications in performing such interactions in a spatially selective manner. We have demonstrated enhanced depth resolution in a microscope setup. With the use of "dark pulses", i.e. pulses which due to quantum interference effects do not interact with an atomic or a molecular system [14] one can generate, for example, a dark nonlinear focus. Spatial polarization control can be used to localize high-harmonic generation, which is a highly polarization sensitive process [15].

Financial support of this research by the Israel Science Foundation is gratefully acknowledged.